Application of post-stack Rune Inversion for reservoir rock properties estimation in comparison with conventional seismic attribute analysis: a case study from the Paleocene formation, Middle Indus basin, onshore Pakistan

Muhammad Zahid Afzal Durrani[1]*, Maryam Talib[1], Vita Kalashnikova[2], Musharaf Sajjad[1], Rune Øverås[2], Carl Fredrik Gyllenhammar[3], Bakhtawar Sarosh[1] and Syed Atif Rahman[1] demonstrate the application of a rune inversion in comparison with the conventional post-stack seismic attributes approach on a Paleocene formation in the Sulaiman Fold belt, Onshore Pakistan and observe good reservoir rock porosity supported by the clay volume and reservoir quality attribute over a potential prospect.

Introduction

Post-stack seismic is stacked seismic traces or seismic trace at zero offset that can be forward modelled as the convolution of the acoustic impedance reflectivity with the wavelet. Post-stack inversion reverses the forward modelling procedure, allowing us to derive the acoustic impedance (P-impedance=Velocity*Density) (Zoeppritz, 1919). Whereas, pre-stack inversion uses seismic traces at different offsets or angles, that extend rock properties estimation to elastic ones like shear impedance (S-impedance=Shear Velocity*Density) and density (Aki-Richards, 1980). Commonly, Zoeppritz and Aki-Richards equations and their approximations are used for deterministic inversion which does not sufficiently resolve density parameter (e.g. Shuey, 1985; Smith and Gidlow, 1987; Fatti et al., 1994; Verm and Hilterman, 1995). Computationally extensive stochastic inversion gives better vertical resolution; however, it requires good data qualifications and the results are anyway an average to deterministic approach (B. Russell, CGG internal methods).

In this study, we tested a novel post-stack inversion approach called 'Rune Inversion (RI)' to estimate reservoir rock properties of Paleocene formation in Sulaiman Foldbelt, Onshore Pakistan. RI uses an artificial intelligence (AI) process, where the base of the algorithm is simulated annealing (Khachaturyan et al., 1979) and global optimizations (Neumaier, 2004) to achieve reasonable rock properties through P-impedance, velocity (Vp) and density (Dn). It requires post-stack seismic data and initial models that are velocity (e.g., seismic velocity) and density. The density model can be computed by converting the velocity field using e.g. Gardner's equation (Gardner et al., 1974). Then, it generates artificial kinematic constraints which are then used to estimate density and velocity iteratively throughout the algorithm.

Using RI, we observed a good separation for Vp and Dn for post-stack seismic data at the Paleocene (LRK) formation.

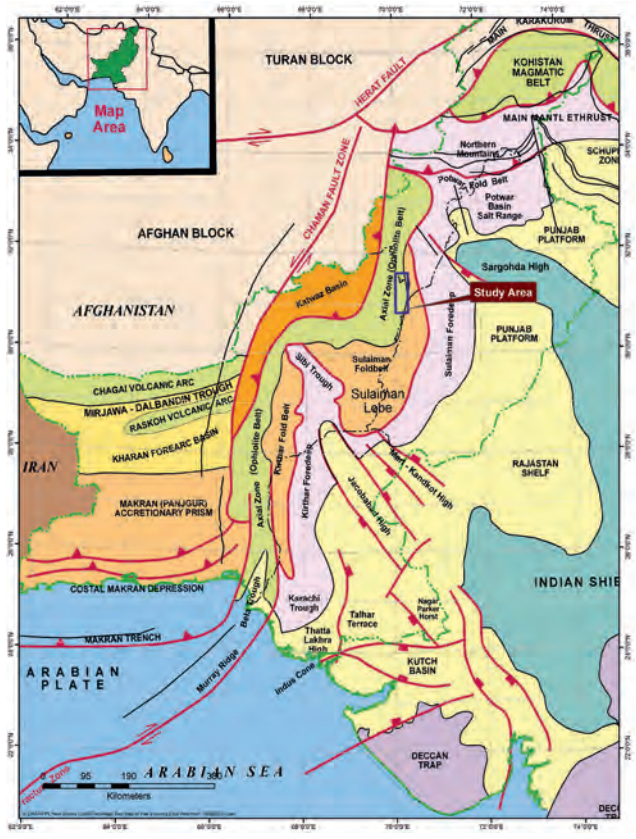

Figure 1 Tectonic map of Pakistan, showing the location of the field under study in Sulaiman fold belt.

[1]Pakistan Petroleum Limited (PPL) | [2]Pre Stack Solutions-Geo AS | [3]Independent consultant, CaMa GeoScience
* Corresponding author, E-mail: m_durrani@ppl.com.pk
DOI: 10.3997/1365-2397.fb2020049

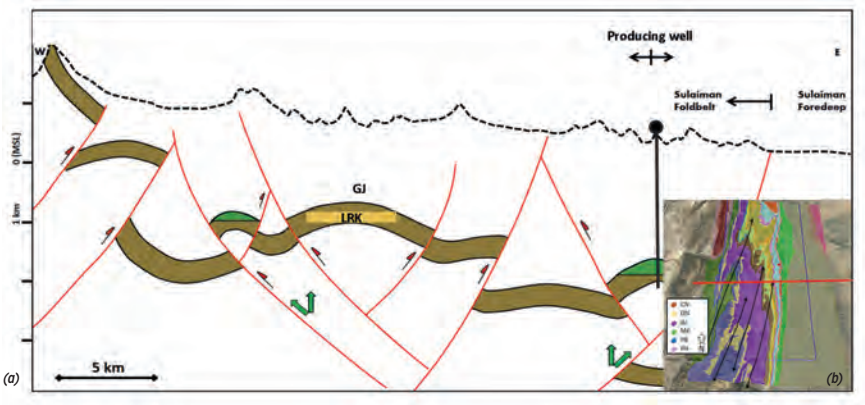

Figure 2 a) Regional cross-section showing different tectonic events in the Paleocene formation and b) generalize lithology illustration in the area.

We demonstrated conventional post-stack seismic attributes (amplitude envelope and sweetness) in comparison with the attributes expressed from RI as an alternative for indirect seismic data analysis. Two wells close to the 3D seismic survey were further used to establish a link between elastic and petrophysical properties (P-impedance and porosity) and as a quality control by comparing well logs information with the predicted rock properties by RI. With limited exploration data, proposed work yields good potential in the LRK formation with good reservoir quality which can be used in pre-drill evaluation.

Regional geological setting, stratigraphy and petroleum system

The field under study lies at the eastern margin of the Sulaiman fold and thrust belt, close to the collision of the Indian plate with the Eurasian plate.

Regionally, multiple fold trends can be marked on the seismic data which are oriented in a NE-SW direction. A regional cross-section shows different tectonic events in the LRK formation where the orientation of the folding trend correlates with the tectonic movement (Figure 2). All these anticlines are cored by Cretaceous rock in the south which progressively becomes younger towards the north.

The stratigraphy of the Sulaiman basin is the result of different tectonic episodes which, beginning from the pre-Cambrian, may be divided into five stages: cratonic inland basin growth stage, continental margin depression stage, rift growth stage, passive continental margin stage and foreland basin growth stage. The stratigraphy of the field under study is established from the nearby wells data and depositional models. The penetrated formations range in age from the Late Jurassic period to more recently (Figure 3). The source rocks in this area are SR and MK formations of Cretaceous age. Reservoirs in this field are primarily PB and LRK sands of Cretaceous and Paleocene age. Shales of LRK and GJ act as the seals for these reservoirs. Paleocene LRK sands, the primary target for this study, are producing hydrocarbons in the nearby fields. These sands are deposited in the marine environment of shallow depth with a prominent influx of clastic having average porosity of 11%. That is why these sands are considered as having reservoir potential after detailed analysis based on the available data.

Conventional seismic attributes analysis

Seismic attributes are the components of the seismic data, which are the quantitative assessment of the seismic characteristics of the interest (Sheriff, 2002; Coren et al., 2001; Chopra and Marfurt, 2005). Seismic attributes analysis of 3D seismic data provides a great opportunity to map seismic anomalies correlating with the geological setting without any well data available (Chen and Sidney, 1997). Earlier, amplitude and frequency dependent attributes have been used as a reconnaissance analysis of the field to evaluate the structural interpretation and reservoir properties in terms of acoustic impedance, reflection coefficient, fluid content (Taner, 2001, Brown, 2001, Chopra and Marfurt, 2005). These attributes could only be valuable when supported with other geological and geophysical inputs to properly model and characterize a reservoir. The purpose of the attributes assessment here is to review some useful seismic attributes (amplitude envelope and sweetness) with the aim to extract subsurface hydrocarbon anomalies (e.g., bright spots) corresponding to depositional elements (fluvial system elements e.g., channel bodies or sand layers) due to an acoustic impedance contrast.

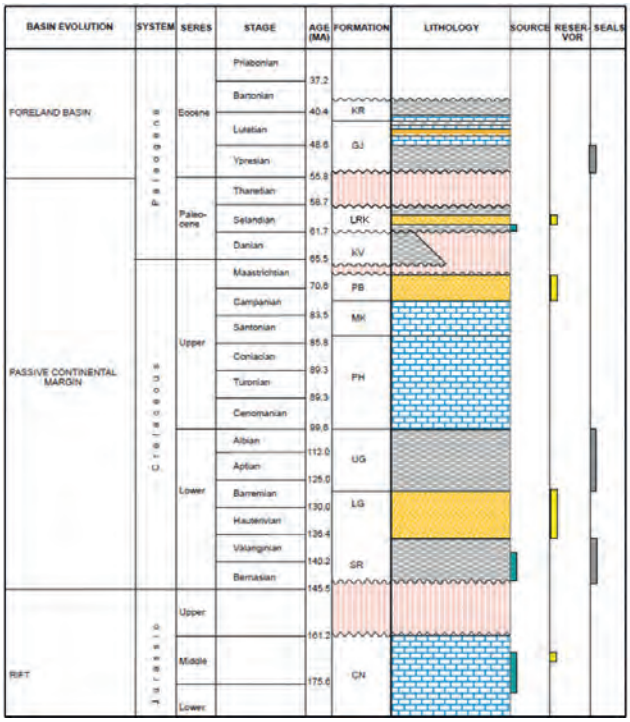

Figure 3 Stratigraphy and petroleum system of the field.

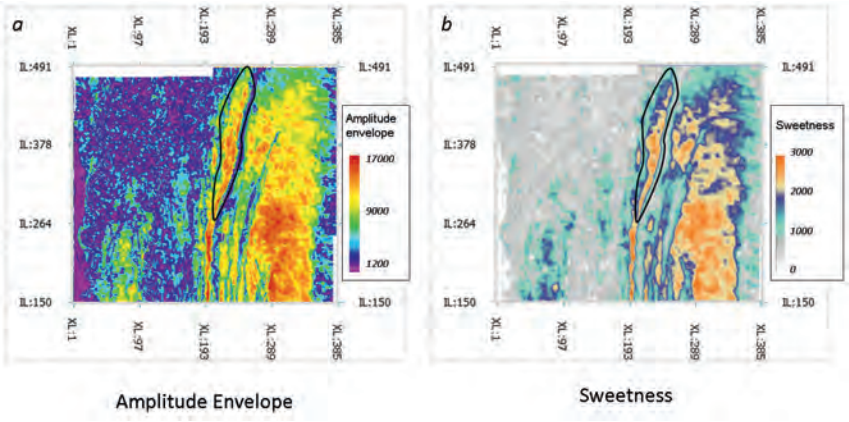

Figure 4 Conventional seismic attributes analysis at the LRK horizon; a) Amplitude envelope, b) Sweetness

Amplitude envelope

Amplitude envelope (reflection strength) is the instantaneous energy of a signal which is proportional to reflection coefficient. This envelope attribute is computed by taking the square root of the sum of the squares of the real and imaginary components, and phase comes from the double argument (ATAN2) inverse tangent of the imaginary and real components, and frequency is computed from the rate of change of the phase (Chopra and Marfurt, 2005). It is the most common popular trace attribute, sensitive to changes in acoustically strong (bright) events on seismic data. It is basically extracted from complex trace by formula (Taner et al., 1979):

$$A(t) = \sqrt{S^2(t) + H^2(t)} \quad (1)$$

Where, A(t) is the amplitude envelope, S(t) is seismic trace and H(t) Hilbert's transform of S(t). There is no effect of phase or polarity on the amplitude envelope as brightness of reflections depend on both phase and polarity. It is helpful in highlighting major changes in depositional environment, unconformities (discontinuities), faults, thin-bed tuning effects and possible hydrocarbon (gas) accumulation.

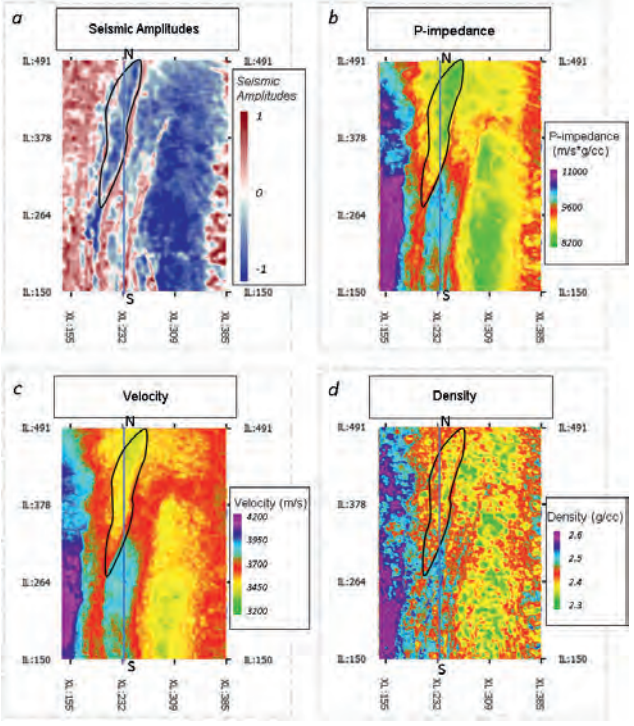

Figure 5 Maps of post-stack Rune Inversion results for LRK horizon + 20 ms (arithmetic mean). Cross-section for XL-235 (blue line) showed in Figure 6; (a) Seismic amplitudes, (b) P-impedance, (c) Compressional velocity, and (d) Density.

Sweetness

Sweetness attribute is the composite attribute and calculated by dividing the amplitude envelope with square root of instantaneous frequency (Taner et al., 1979). Mathematically it can be written as:

$$Sweetness = \frac{A(t)}{\sqrt{F(t)}} \quad (2)$$

where, F(t) is the instantaneous frequency.

The sweetness attribute is very helpful in imaging thick sand intervals and provides initial idea about sweet spots that are hydrocarbon (oil and gas) prone (Radovich and Oliveros, 1998). It is very useful in thick, isolated and clean reservoir bodies because of stronger reflections than surrounding and less useful in thin, interbedded reservoirs because of low acoustic impedance contrast (Hart, 2008). The sweetness attribute reduces the influence of high frequency events so that higher amplitude and lower frequency areas (sweet spots) show the highest value for sweetness (Koson, 2013).

Figure 4 shows the data slices for amplitude envelope and sweetness attributes at the LRK horizon. There is an indication of brightening of amplitude with higher values for sweetness attribute at a pop-up structure (highlighted in black) with four-way closure that can be mapped on seismic data. To the east of this structure, there is an exposed anticline which is also depicting higher values for the sweetness attribute. However, to gain more confidence in estimation, there is a need to validate these attributes in conjunction with other methods to further de-risk the prospect. As there is no well data available inside the 3D seismic, but available outside the 3D seismic coverage on 2D seismic sections with very weak well to seismic ties, it was unreliable to perform deterministic post-stack or pre-stack inversion. Therefore, Rune Inversion was chosen to be tested as the only possibility to estimate rock physical parameters.

Post-stack Rune Inversion and its application on the LRK Formation

The main idea behind the proposed Rune Inversion algorithm is to characterize the areas where there are no well logs and seismic gathers data available and despite the lack of data it is still possible to estimate elastic rock properties. Post-stack RI is an artificial intelligence inversion algorithm, which allows for estimating velocity and density separately from post-stack seismic and seismic velocity data with no well logs data required. It provides a good link between geology and geophysics. The base of the RI are artificial kinematics constraints, simulated annealing (Sen and Stoffa, 1991) and global optimizations (Ma, 2002; Goffe et al., 1994) algorithms. As in any other inversion algorithm, RI also requires a seismic zero phase control. There is no coupling between velocity and density beyond frequency of the initial models in RI. The better quality of seismic and seismic

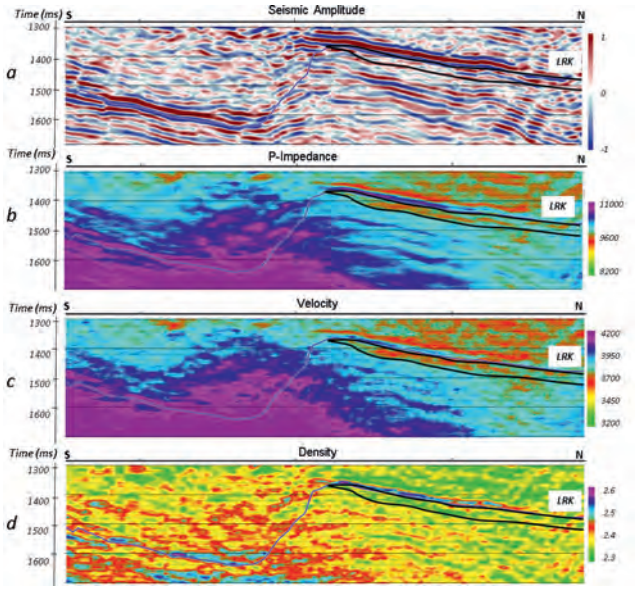

Figure 6 Cross-sections of post-stack Rune Inversion results passing though proposed DNW well location (dashed white line), base map is on figure 5; (a) Seismic data, (b) P-impedance, (c) Compressional velocity, and (d) density.

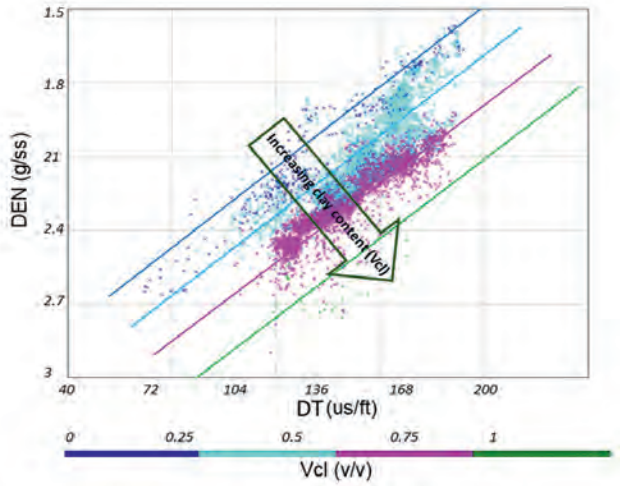

Figure 7 Sonic (DT) – density (DEN) cross-plot coloured with volume of clay (Vcl). The blue colour represents clean sands while the green colour represents more than 75% clay content in the rock.

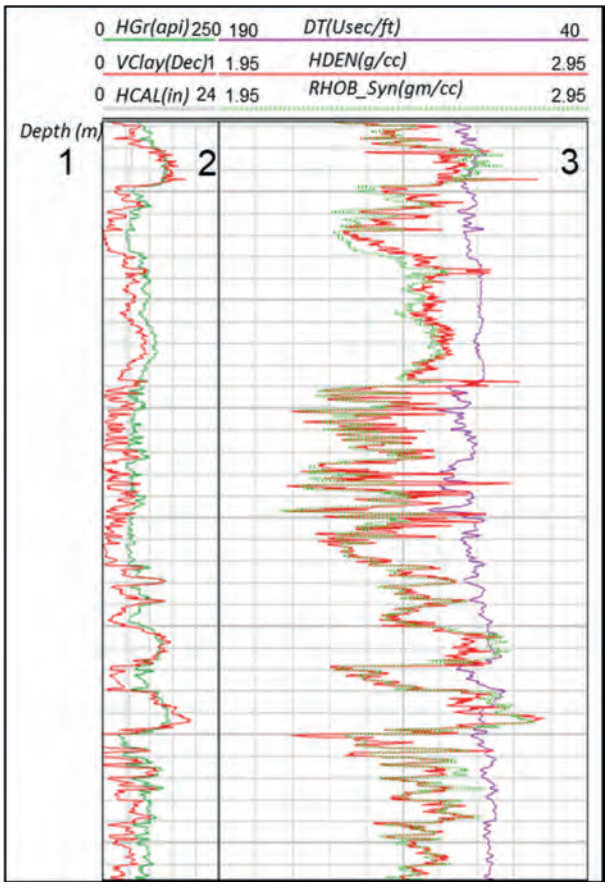

Figure 8 Synthetic and real logs comparison. In track 2 – Gamma Ray (GR) curve is in green and the volume of clay (Vcl) is in red. In track 3 – the green dashed curve is the synthetic density, whereas, the recorded density curve is in red and the sonic curve is represented by a violet colour.

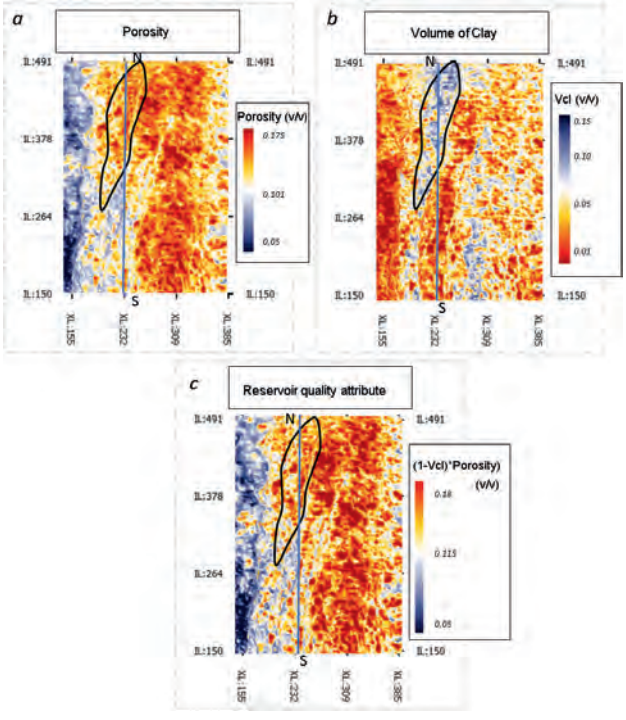

Figure 9 Maps of recomputed physical rock properties from RI results for LRK horizon + 30 ms (arithmetic mean). Cross-sections for the blue X-line are shown on Figure 10; (a) Porosity, (b) Volume of clay, and (c) Reservoir quality attribute.

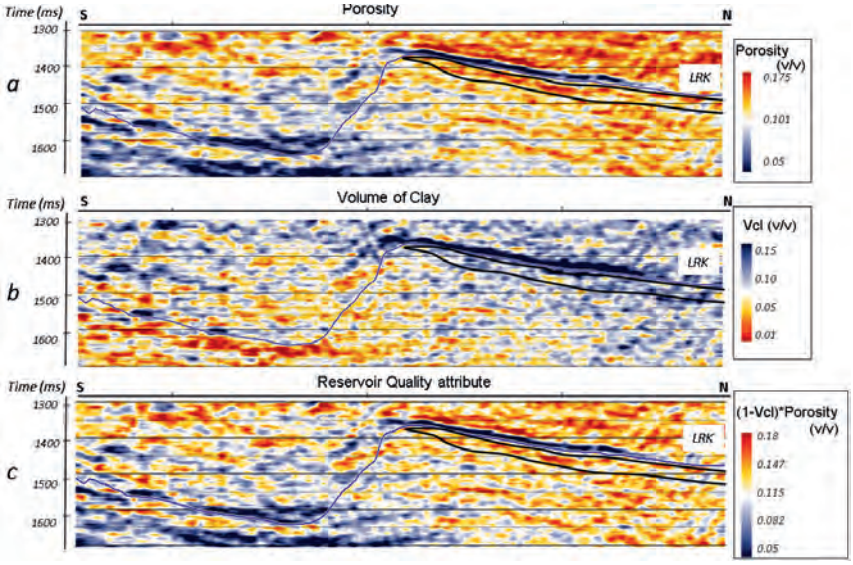

Figure 10 Cross-sections of recomputed physical rock properties from RI results, base map is on Figure 9; (a) Porosity, (b) Volume of clay, and (c) Reservoir quality attribute.

velocities, the faster and more accurate separation of density and velocity can be achieved. Compared to conventional post-stack and pre-stack inversion of deterministic approach, RI yields more reliable density, because it does not have any coupling between velocity and density.

We tested RI on a frontier onshore field in Middle Indus basin of Pakistan, which does not have any well data information available inside the 3D seismic coverage. Available seismic velocity was converted to a density field by using Gardner's equation. Then, seismic velocity and produced density fields were used as initial models. Studied seismic data was checked for zero phase at the formation interest. Post-stack seismic data and initial models were then used in RI to invert for elastic properties (P-impedance, density and velocity). Further, the produced volumes were used to characterize the reservoir petrophysical properties (porosity and volume of clay) and 'reservoir quality' attribute.

Figure 5 shows the maps of post-stack seismic amplitudes, post-stack RI inverted P-impedance, velocity and density for LRK horizon. A decrease in P-impedance, velocity, and density could be seen at the target structure. Moreover, this decrease in properties remains the same towards northern plunge which could increase the chance of additional hydrocarbons accumulation due to tilted gas water contact (GWC). The observed

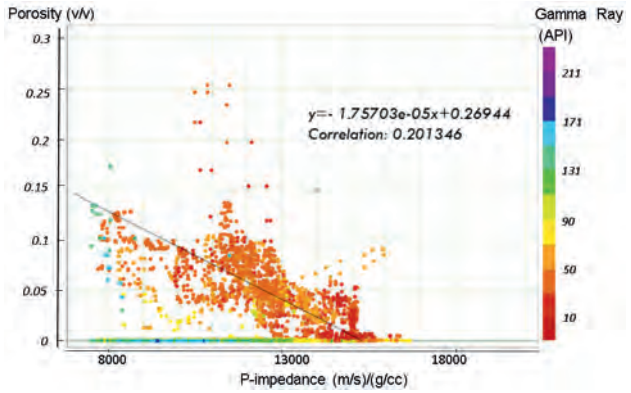

Figure 11 P-impedance versus effective porosity relation derived from the nearby wells.

P-impedance varies around 8000-9000m/s*g*cc from the RI estimation, while the average P-impedance from the nearby well logs at the same formation is about 9000-12000m/s*g/cc. Similar comparison was observed for density and velocity: Dn ~ 2.37g*cc (by RI), Dn ~ 2.3–2.5g*cc (logs), velocity ~ 3450m/s (by RI), Vp – 4500-5200m/s (logs). Therefore, we can see a reasonable estimation of rock properties produced by RI algorithm.

Inversion derivatives

In the petrophysics world, the first parameter to determine in a sedimentary environment mainly composed of sand (quartz) and clay minerals is the volume of clay (Vcl) versus the volume of sand (1-Vcl). There are several methods to calculate Vcl such as gamma ray (GR) log, density-neutron and DT-density relationship. Figure 7 is a typical DT-DEN cross plot where dark blue samples represent Vcl less than 25% and green samples represent Vcl above 75%. This plot shows that there is a linear relationship between velocity and density and volume of clay. Using the graphical illustration of Figure 7, the parameters of density (DEN), velocity (DT) and Vcl can be expresses as

$$\mathrm{DEN} = a\mathrm{Vcl} + b - \left(c\mathrm{DT}\right), \tag{3}$$

where DEN is a density, Vcl is a volume of clay, DT is a sonic log, a is a function of compaction, and b and c are the functions of the sedimentary basins (Gyllenhammar, 2016 and 2020).

Figure 8 shows the precision that can be obtained using this methodology. Calculated Vcl using the DT-DEN relationship is shown on track 2, Figure 8. The resulting synthetic density curve (track 3) is not simply mimicking the sonic curve, but overlies the actual density curve quite well.

Using this methodology, we recomputed the inverted volumes of velocity and density by RI to the volume of clay and porosity (Figure 9). Porosity volume has been computed using the below formula:

$$Dn = \varphi_1\rho_{fl} + \left(1-\varphi_1\right)\left(V_{cl}\rho_{clay} + \left(1-V_{cl}\right)\rho_{sand}\right. \tag{4}$$

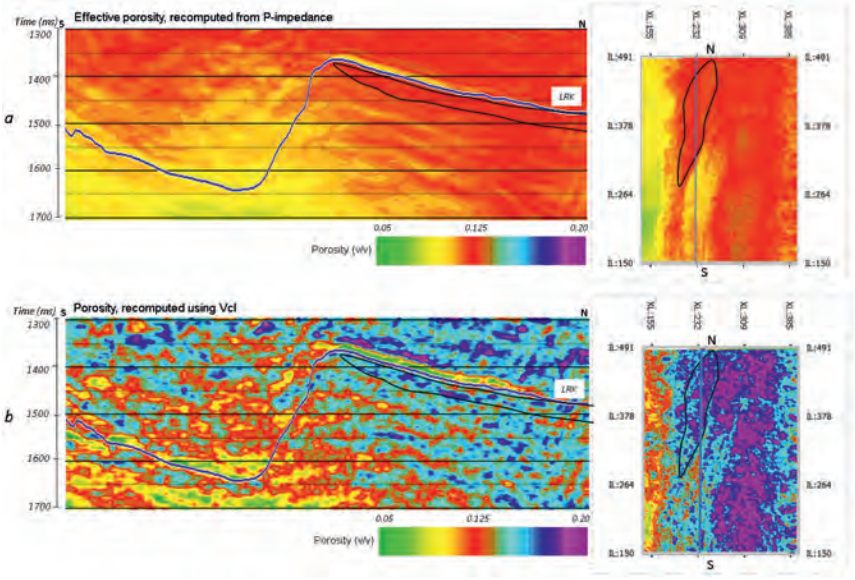

Figure 12 Comparison of Porosity cross-sections along the X-line displayed (in blue) on the data slices extracted over LRK using; (a) statistical regression equation from P-impedance and (b) alternative methodology from RI-inverted velocity and density.

where ρ_{clay} – is a density of clay minerals, ρ_{sand} – is a density of the quartz, and ρ_{fl} is a density of fluid equal to 1g/cc. We assume that the water saturation is 100%, ρ_{sand} is 2.65 g/cc and ρ_{clay} is 2.58g/cc, and the media is of normal compaction and no erosion. Further, reservoir quality attribute has been computed – a good porosity sandstone as:

$$Reservoir\ \ Attribute = (1 - Vcl) * \varphi, \quad (5)$$

where φ is the total porosity computed from the inverted density volume (4).

We observed good porosity of an average 13-17% at the LRK formation in the highlighted zone in black (Figures 9 and 10). Even though the estimated volume of clay remains high along the structure, the reservoir quality attribute shows a good potential for reservoir presence at the LRK formation.

Porosity prediction methods comparison

Post-stack P-impedance estimated by RI is comparable to conventional deterministic post-stack inversion (V. Kalashnikova, PSS-Geo internal methods, April 2019). We computed porosity as it would be computed having only a P-impedance volume from conventional post-stack inversion, to compare with porosity estimated from derivatives of RI over the LRK formation. For conventional porosity estimation, a statistical regression relation has been generated from nearby wells data and applied on the P-impedance volume to model effective porosity (Figure 11).

Porosity computation based on the inverted P-impedance shows the comparable variation response (along the LRK formation) and as it is expected based on stratigraphic analysis and petrophysical data (Figure 12). RI gave slightly higher absolute values of porosity (~18%) and, overall, better resolution. The variations of absolute values can be explained in conjunction with the predicted volume of clay (Figures 9 and 10), that gives a better understanding of formation media to propose a well location.

Discussion

Post-stack seismic data is widely available, but even with the latest techniques and machine resources have not been used broadly. AVO and pre-stack seismic inversion took over to produce estimation of rock properties. Mega grids of post-stack data which are not suitable for pre-stack studies or vintage post-stack data can still be utilized through extracting more value from it. Artificial intelligence algorithms can help to solve the problems that were previously impossible, and enable us to review the data that was left as doubtful.

Separation of density and velocity is a challenging process for any inversion. Rune Inversion produces independent velocity and density and comparable P-impedance to conventional algorithms. In addition, using proposed alternative methodology for density estimation as a function of clay and velocity makes it possible to produce reliable reservoir attributes such as porosity, a volume of clay, and reservoir quality using post-stack seismic data. For the demonstrated example on the RI application, we used simple porosity computation from density. However, having a volume of clay in hand to reduce uncertainty in porosity prediction it is also possible to compute porosity using Hashin-Shtrikman and Gassmann approaches. Then, averaging both approaches, we can get an estimation that is more reliable. In the case of LRK formation, we saw similar porosity estimations; therefore, we presented only one approach.

Another interesting aspect of the Rune Inversion is that the combination of derivatives can be used as an alternative to AVO attributes. For example, conventional Fluid Factor (Fartti et al., 1994) can be replaced with $Vp/Vp_{initial\_model}$ and $Dn/Gardner(Vp_{initial\_model})$. At Fluid Factor, we look for a decrease in compressional reflections compared to shear reflections with correction to a mudrock as an indicator of possible hydrocarbon presence. In Rune Inversion, we look for density drops radically compared to surrounding media. Radical drops in density may indicate porous rocks or rocks filled with hydrocarbons. That, again, gives an additional quick evaluation of the prospect without pre-stack data and resourceful tools.

Relative inversion

We demonstrated absolute inversion in this article. When no reliable initial models of velocity and density can be constructed,

e.g. seismic velocity is really of bad quality and no well logs are available to construct the initial velocity model, it is possible to compute a relative inverted P-impedance, density, velocity and Dn/Gardner ($Vp_{initial\_model}$) attribute. These relative inverted volumes and attributes can give a better understanding of rock properties distribution and help to evaluate fluid possible accumulation.

Conclusion

Rune Inversion is the first seismic inversion that is fully based on artificial intelligence algorithms and was originally developed to characterize post-stack data (without any wells information) to produce reasonable estimates of the most convenient reservoir rock properties: P-impedance, Velocity, and Density. We showed its application on a Paleocene LRK formation in the Sulaiman Foldbelt, Onshore Pakistan. The elastic properties proved to be more appropriate along with the conventional seismic attributes reconnaissance analysis for the evaluation for hydrocarbon exploration. Using inverted P-impedance and density output, porosity was computed in two ways: using statistical regression equation generated from nearby wells log information, which are comparable to the expected rock properties of the LRK formation based on stratigraphic analysis and petrophysical data, and porosity from density. Both showed comparable results, where porosity from density had better resolution. The new approach of volume of clay computation from density and velocity accompanied porosity and reservoir quality attribute analysis helped in understanding reservoir rock properties variations. Overall, RI derivatives and attributes are a great step forward in working with post-stack data. It helps to see rock properties distribution that was not possible before. Rune Inversion proved to be a reliable first quick estimation of possible reservoir properties distribution in conjunction with conventional seismic attribute analysis, which also supports the Rune post-stack inversion results.

Acknowledgements

We wish to thank Pakistan Petroleum Limited (PPL) and Partner (Zhenhua Oil Co.) management for granting the permission to publish the study data. We would also like to acknowledge Pre-Stack Solution Geo (https://www.pss-geo.com/) officials; Vita Kalashnikova and Rune Øverås, for their technical support in this study.

References

Aki, K. and Richards, P.G. [1980]. *Quantitative Seismology: Theory and Methods*. V.1, W.H. Freeman and Co.

Brown, A.R. [2001]. Understanding seismic attributes. *Geophysics,* **66**(1), 47-48.

Chen, Q. and Sidney, S. [1997]. Seismic attribute technology for reservoir forecasting and monitoring. *The Leading Edge*, **16**(5), 445-448.

Chopra, S. and Marfurt, K.J. [2005]. Seismic attributes - A historical perspective. *Geophysics*, **70**, 3SO-28SO.

Coren, F., Volpi, V. and Tinivella, U. [2001]. Gas hydrate physical properties imaging by multi-attribute analysis – Blake Ridge BSR case history. *Marine Geology,* **178**(1-4), 197-210.

Fatti, J.L., Smith, G.C., Vail, P.J., Strauss, P.J., and Levitt, P.R. [1994]. Detection of Gas in Sandstone Reservoirs Using AVO Analysis: A 3-D Seismic Case History Using the Geostack Technique. *Geophysics*, **59**, 1362-1376.

Gardner, G., Gardner, L. and Gregory, A. [1974]. Formation velocity and density – the diagnostic basis for stratigraphic traps. *Geophysics*, **39**, 770–780.

Goffe, W.L., Ferrier, G.D. and Rogers, J. [1994]. Global optimisation of statistical functions with simulated annealing. *Journal of Econometrics*, **60**, 65–100.

Gyllenhammar, C.F. [2016]. Is there space for petrophysics in Rock Physics? Conference abstract. *New Advances in Geophysics (NAG) meeting*, Abstracts.

Gyllenhammar, C.F. [2020]. Calculating a synthetic density curve using a volume of clay and velocity. *First Break*, **38** (6), 45–49.

Hart, B.S. [2008]. Channel detection in 3-D seismic data using sweetness. *AAPG bulletin*, **92**(6), 733-742.

Kalashnikova, V. [2019]. *PSS-Geo internal methods*, April 2019, retrieved from www.pss-geo.com/runeinversion

Khachaturyan, A., Semenovskaya, S. and Vainshtein, B. [1979]. Statistical-Thermodynamic Approach to Determination of Structure Amplitude Phases. *Sov.Phys. Crystallography*, **24**, 519-524.

Koson, S. [2013]. *Enhancing geological interpretation with seismic attributes, Gulf of Thailand.* Chulalonkorn University.

Ma, Z.Q. [2002]. Simultaneous inversion of Pre-Stack seismic data for rock properties using simulated annealing. *Geophysics*, **67**, 1692-2041.

Neumaier, A. [2004]. Complete Search in Continuous Global Optimization and Constraint Satisfaction. In: Iserles, A. (Eds.) *Acta Numerica*, Cambridge University Press.

Radovich, B.J. and Oliveros, R.B. [1998]. 3-D sequence interpretation of seismic instantaneous attributes from the Gorgon Field. *The Leading Edge*, **17**(9), 1286-1293.

Russel, B. [2019]. *Stochastic vs Deterministic Pre-stack Inversion Methods*. Retrieved from https://www.cgg.com/data/1/rec_docs/3414_3412_Stochastic_vs_Deterministic_Inversion_Russell.pdf.

Sen, M.K. and Stoffa, P.L. [1991]. Nonlinear one-dimensional seismic waveform inversion using simulated annealing. *Geophysics*, **56**, 1624-1638

Sheriff, R.E. [2002]. Encyclopedic dictionary of applied geophysics. *Society of Exploration Geophysicists,* Tulsa, USA.

Shuey, R.T. [1985]. A Simplification of the Zoeppritz Equations. *Geophysics*, **50**, 609-614.

Smith, G.C. and Gidlow, P.M. [1987]. Weighted stacking for rock property estimation and detection of gas. *Geophysical Prospecting*, **35**, 993-1014.

Taner, M.T., Koehler, F., and Sheriff, R. E. [1979]. Complex seismic trace analysis. *Geophysics*, **44**(6), 1041-1063.

Taner, M.T. [2001]. Seismic attributes. *Canadian Society of Exploration Geophysicists Recorder,* **26** (7).

Verm, R. and Hilterman, F. [1995]. The calibration of AVO cross plotting to rock properties. *The Leading Edge*, **14**, 847-853.

Zoeppritz, K. [1919]. VIIb. Über Reflexion und Durchgang seismischer Wellen durch Unstetigkeitsflächen. *Nachrichten von der Königlichen Gesellschaft der Wissenschaften zu* Göttingen, *Mathematisch-physikalische Klasse*, 66-84.

FIRST BREAK

VOLUME 38 | ISSUE 7 | JULY 2020

SPECIAL TOPIC

Machine Learning

EAGE
EUROPEAN ASSOCIATION OF GEOSCIENTISTS & ENGINEERS